

PAPER • OPEN ACCESS

Verification of a calibration method for 3D screw thread metrology

To cite this article: A Przyklenk *et al* 2021 *Meas. Sci. Technol.* **32** 094005

View the [article online](#) for updates and enhancements.

You may also like

- [A method for detecting alignment deviation on a thread-measuring instrument](#)
Sheng Chen, Dongbiao Zhao, Yonghua Lu et al.
- [Analysis on screw preload condition of acoustic beacon in high water pressure environment](#)
Yang Chen, Shichao Dong, Junbo He et al.
- [Simulation and Analysis of Screw Thread based on Workbench](#)
Shanshan Zhang, Qionghua Yu, Ding Ding et al.

Verification of a calibration method for 3D screw thread metrology

A Przyklenk^{1,*} , S Schädel²  and M Stein¹ 

¹ Physikalisch-Technische Bundesanstalt (PTB), Bundesallee 100, 38116 Braunschweig, Germany

² ZEISS Industrial Metrology, Carl-Zeiss-Straße 22, 73447 Oberkochen, Germany

E-mail: anita.przyklenk@ptb.de

Received 24 November 2020, revised 2 February 2021

Accepted for publication 1 March 2021

Published 1 June 2021



CrossMark

Abstract

The novel approach for holistic screw thread calibrations developed by the Physikalisch-Technische Bundesanstalt was published in 2019. A significant achievement has been made in order to meet increasing demands in manufacturing processes and quality assurance, particularly when workpieces with complex geometries are under inspection. This article deals with the verification of the previously presented three-dimensional calibration procedure for screw threads. Screw thread pitch diameters, the lead and flank angles are compared to those determined by the standardized method based on line-like, rather two-dimensional measurements and evaluation. In order to provide a reliable basis for the verification, one thread gauge was calibrated under laboratory conditions for precision metrology. Additionally, calibrations were conducted by three alternating operators on three different coordinate measuring machines to investigate the influence by user and machine. The resulting normalized errors $|E_n|$ of screw thread determinants under test and reference values are significantly smaller than 0.5 which indicates a high level of agreement.

Keywords: screw thread metrology, coordinate measuring technology, 3D evaluation algorithm, local screw thread determinants, verification

(Some figures may appear in colour only in the online journal)

1. Introduction

Screw threads are frequently used machine elements within highly developed mechanical applications. Principal functions of screw threads are to fasten, connect, seal or centre parts. Due to increasing requirements on function and reliability, manufacturing tolerances are constantly decreasing. In accordance with current standards [1–3] and calibration guidelines [4–7], the evaluation of screw thread determinants is carried out by gathering 2D coordinates in two defined axial sections. Following the conventional procedure, fundamental form deviations cannot be figured out due to the limited number of

gathered points. For example, roundness deviations cannot be detected and, harmonic form deviations caused by tool vibrations cannot be measured at all. Furthermore, the results require a high degree of interpretation. For instance, pitch diameters which are smaller than nominal values can be caused either by concave flanks or by a stylus ball diameter which is smaller than the optimum sized one. Therefore, the complex geometry of screw threads is insufficiently evaluated regarding its functionality and requirements for quality assurance. Hence, the calibration strategy needed to be adapted.

There is also an imbalance between the available measuring systems and the standardized measuring strategy. While measuring systems enable increasingly precise results [8, 9], the accuracy of metrology according to current calibration guidelines still depends on the operator and systematic errors [10–12]. Effort has been made to include novel technologies for enhanced screw thread metrology. For instance, an approach to perform screw thread calibrations by means of optical measurements on coordinate measuring

* Author to whom any correspondence should be addressed.



Original Content from this work may be used under the terms of the [Creative Commons Attribution 4.0 licence](https://creativecommons.org/licenses/by/4.0/). Any further distribution of this work must maintain attribution to the author(s) and the title of the work, journal citation and DOI.

machines (CMMs) is suggested [13]; a charge-coupled device camera system for fast inspections of internal screw threads in industrial applications is proposed [14] and a method for the inspection of screw thread determinants obtained from computed tomography measurements is developed [15]. However, a variety of custom-made systems and commercial CMMs is used for screw thread metrology [16], where two trends can be identified. On the one hand, optical methods are rather performed with the aim of fast calibrations and a few with consideration of an area-based measuring strategy but without achieving the accuracy that can be obtained by tactile probing [17]. On the other hand, tactile methods are used on high-precision CMMs but only for 2D inspections [18] according to the current calibration guideline [4].

The developments presented in [19] were carried out under consideration of central aspects of the ‘Manufacturing Metrology Roadmap 2020’ published by the German VDI/VDE Society for Measurement and Automatic Control (GMA) in 2011 [20, 21]. In particular, a reduced time effort of inspections is aimed for. Another goal is an increased accuracy and flexibility. Regarding these requirements, the Physikalisch-Technische Bundesanstalt (PTB) has developed a calibration procedure for screw threads based on a mathematical 3D model of the screw thread geometry [19].

A detailed description of the theoretical fundamentals of the calibration procedure investigated here is published in [19]. An explicit description for the determination of local pitch diameters is given in [22].

In this paper, the verification of the novel 3D screw thread calibration method is presented. In order to validate the new procedure, the consistency of 3D and 2D measuring results is investigated. Regarding a reasonable comparison, one screw thread gauge is calibrated with both methods under laboratory conditions for high precision measurements. In addition, the user influence of the novel 3D method is analysed. Therefore, measurements are conducted on three CMMs by three operators. Based on the 3D screw thread calibration method investigated in the following, novel and improved metrological services for screw thread standards will be offered and performed by the PTB in the future.

Section 2 gives a brief introduction into the 2D standardized thread calibration method. Section 3 introduces the key aspects of the 3D approach for holistic screw thread calibrations. Section 4 deals with the enhanced verification of the 3D approach. An outlook and the conclusion is given in section 5.

2. 2D calibration method

The conventional 2D approach for determining the gauge pitch diameter of parallel screw thread measuring machines with mechanical probing using 1D, 2D or 3D CMMs is given in the EURAMET cg-10 Calibration Guide [4].

It is recommended to determine the pitch diameter d_2 following the three-wire method by means of measurements along two specified axial sections A – B and C – D, which are arranged perpendicular to each other, as illustrated in the

top view of a screw thread shown in figure 1(a). Figure 1(b) shows the side view A – B of a cylindrical external screw thread with asymmetrical profile. The pitch diameter d_2 is determined based on measurements in at least three different transverse sections. In these planes, tactile probing in two-point-contact with calibrated spherical or cylindrical geometry elements is carried out to determine the indicated value m , as shown in figure 1(c). From the centre coordinates of each triplet (R1, R2 and L2) measured in one axial section along one screw thread, the indicated value m is easily calculated. The optimum diameter of the stylus ball d_D depends on the nominal screw thread geometry. Assuming that d_D , the pitch P and the screw thread angle α are known, the pitch diameter d_2 of an external screw thread with symmetrical flank angles $\beta = \gamma = \alpha/2$ can be calculated knowing the indicated value m :

$$d_2 = m - \frac{d_D}{\sin\left(\frac{\alpha}{2}\right)} + \frac{P}{2} \cdot \cot\left(\frac{\alpha}{2}\right) - A_1 + A_2, \quad (1)$$

where A_1 denotes a rake correction term and A_2 considers contact forces during the probing process. The calibration guideline [4] does not give any recommendation for the inspection of the lead of helix Ph , the pitch P , the screw thread angle α and the flank angles β and γ . However, for single-start screw threads, the lead of helix Ph and the pitch P are equal and result from distances in the direction of the z -axis measured by consecutive two-point-contact probing in one axial section. The probing is illustrated with stylus spheres L1 and L2 on the left hand side and with R1 and R2 on the right hand side in figure 1(c). P should be determined in both axial sections A – B and C – D. The determination of the flank angles α , β and γ is usually conducted by contour measurements with pointed tip styli in the direction of the screw thread axis in both axial sections.

3. 3D calibration method

This section gives a brief overview of the applied 3D screw thread calibration method. A detailed description of the procedure is given in [19, 23]. The applied calibration applies to parallel or tapered internal and external multi-start screw threads. However, this article deals with cylindrical single-start external screw threads. Holistic inspections by tactile probing on commercial CMMs are proposed to quantify all thread determinants from one measured point cloud in one reference coordinate system. Herein, following aspects are taken into account:

- Definition of a geometrical ideal form element of a screw thread.
- Concept of an area-based measurement strategy.
- Holistic evaluation of the measured point cloud.
- Estimation of uncertainties by means of the Monte Carlo Method.

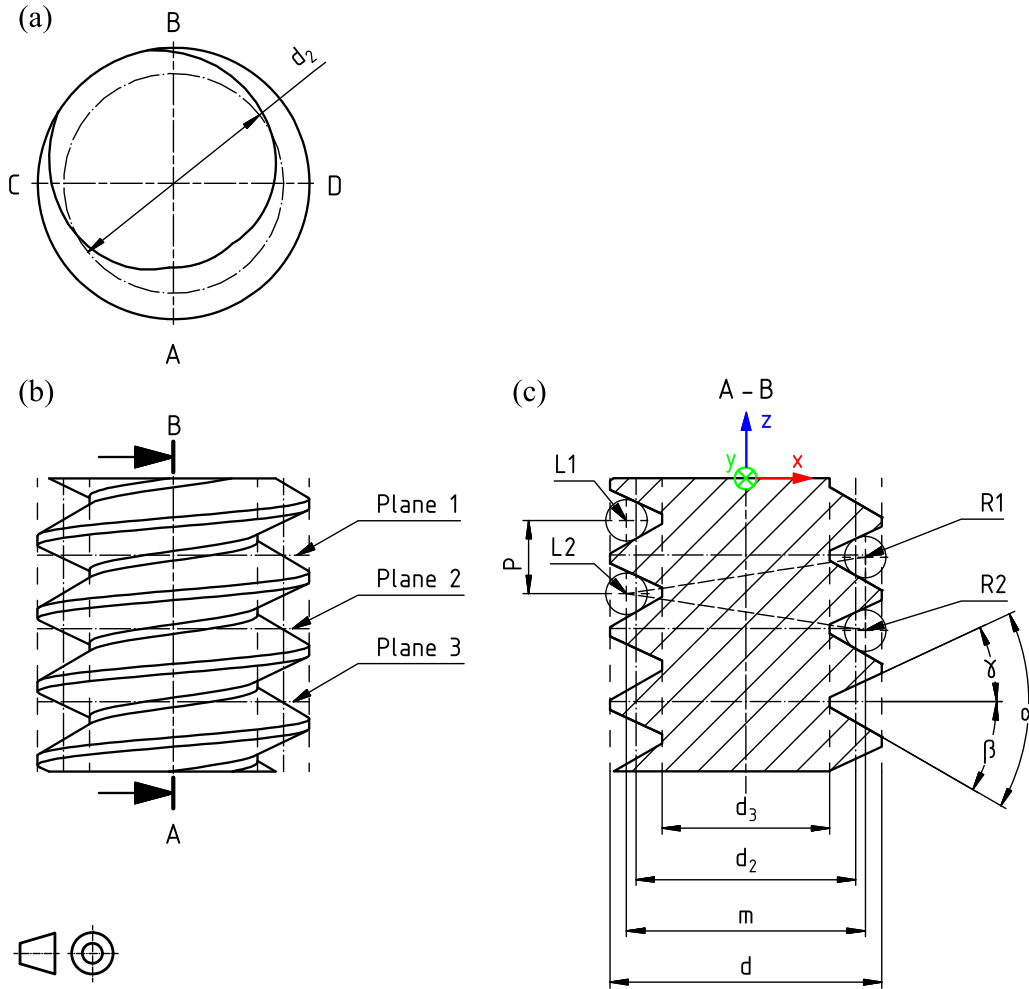


Figure 1. Technical drawing of a cylindrical external screw thread with asymmetrical profile to demonstrate the 2D measuring strategy according to the calibration guideline EURAMET cg-10. (a) Top view with axial sections of inspection A – B and C – D. (b) Side view with the minimum number of specified planes for inspection. (c) Axial section with all screw thread determinants. The spanned triangle between points R1, R2 and L2 illustrates the three-wire method for the determination of pitch diameter d_2 .

3.1. Geometrically ideal form element of a screw thread and the pitch diameter

The geometrically ideal form element of a screw thread is parametrised as presented in [19] and consists of two standard screw surfaces S_j with $j = 1, 2$:

$$S_j(u_j, v_j, p_{j1}, p_{j2}) = \begin{pmatrix} x_j \\ y_j \\ z_j \end{pmatrix} = \begin{pmatrix} u_j \cdot \cos(v_j) \\ u_j \cdot \sin(v_j) \\ v_j \cdot p_{j1} + u_j \cdot p_{j2} \end{pmatrix}. \quad (2)$$

$S_j(u_j, v_j, p_{j1}, p_{j2})$ is expressed in Cartesian coordinates and parameterized in cylindrical coordinates with radii u_j and polar angles v_j , where p_{j1} and p_{j2} denote geometry parameters from which the pitch of single flanks:

$$P_{Zj} = 2\pi \cdot p_{j1}, \quad (3)$$

and the flank angles:

$$\beta = \arctan(p_{12}), \quad (4)$$

and

$$\gamma = \arctan(p_{22}), \quad (5)$$

can be derived. All screw thread determinants are based on equations (2)–(5) and a translational degree of freedom t_{Zj} that corresponds to intersections along the z -axis of the screw thread. Then the pitch diameter $d_2(z)$ is obtained by

$$d_2(z) = 2 \cdot \left(\frac{p_{11} - p_{21}}{p_{11} \cdot p_{22} - p_{12} \cdot p_{21}} \cdot z - \frac{p_{11} \cdot t_{Z2} - p_{21} \cdot (t_{Z1} + \pi \cdot |p_{11}|)}{p_{11} \cdot p_{22} - p_{12} \cdot p_{21}} \right). \quad (6)$$

3.2. Area-based measuring strategy

Area-based measuring is performed on bridge-type CMMs with an integrated rotary table (RT) in single-contact scanning mode. The proposed 3D measuring strategy enables a high degree of automation. To perform a 3D calibration, the following steps are required:

- (a) Determination of the workpiece coordinate system.
- (b) Calculation of a nominal point cloud on the basis of the previously defined form element in parameter representation (equation (2)), taking into account the coordinates measured in step 1 and the nominal screw thread parameters.
- (c) Characterization of the RT-axis position and orientation.
- (d) Helix scans on both screw thread flanks in single flank contact on different radii for an independent area-based acquisition of both screw thread flanks in one common reference coordinate system.
- (e) Reversal method to eliminate the influence caused by RT-axis deviations by means of Donaldson's method [24] using one probe for each of the two redundant measurements.
- (d) Traceability to the SI-unit is ensured by means of substitution artefacts or measurement standards.

3.3. Evaluation of measured point clouds

The evaluation of measured point clouds is performed by an algorithm developed by PTB using the approaches of [25] and [26]. In the first step, two nominal form elements S_j with $j=1,2$ representing flank 1 and flank 2 (equation (2)), are adapted by changing the geometry parameters (p_{j1}, p_{j2}) and location parameters (t_{zj}) of the surfaces iteratively for the determination of the best-fitted form element into the actual point cloud. Residuals that occur between form elements and measured point clouds provide information about form deviations. The pitch diameter is calculated simultaneously with equation (6) and is marked with the index l_s , since it depends on the best-fitting form element resulting from the least squares optimization.

In the second step of the evaluation, the influence of form deviations on the required true pitch diameter is quantitatively ascertained by determining local pitch diameters, which are called with the index loc . Local pitch diameters are calculated directly from the actual point cloud by iteratively searching in all measured axial sections for pairwise opposite teeth and grooves of equal length in the direction of the rotation axis. According to the radial coordinates of the pairwise determined segments, local pitch diameters can be assigned to each axial section [23, 27]. Local pitch diameters refer to a shorter reference length than those which are determined in the first evaluation step by means of the ideal form element. They are able to represent the screw thread shape in a more flexible way, which can lead to a more precise reproduction of the true shape, depending on the manufacturing quality. The larger shape deviations are, the larger is the benefit of the additional information about local pitch diameters. Furthermore, the best comparability is given to conventionally derived diameters with the 2D calibration method; which does not mean that the local diameters are generally preferable to least-squares results.

3.4. Comparison to the 2D method

The individual process steps of the 2D and 3D thread calibration are compared figure 2 by means of a flowchart. In order to keep it concise, the individual process steps are organised by

building three groups: preparation, data acquisition and evaluation. The 3D thread calibration procedure, which is shown on the right side, requires more steps than the 2D method to prepare the measurement itself. In contrast to the 2D method, which requires the gauge to be rotated and re-clamped several times by hand, the data are gathered in one step without changing the reference system. Subsequently, the joint evaluation of the point cloud is carried out, from which all thread determinants are derived. The 2D evaluation uses individual measurements and gathered coordinate pairs are evaluated to determine one single thread determinant at a time.

4. Verification of the novel 3D calibration method

In order to verify the novel 3D calibration method of screw threads, the consistency of 3D and 2D inspection results is investigated. Regarding to create a reasonable basis for comparison, one metric external single-start screw thread gauge $M64 \times 6$ (figure 3) is calibrated with both methods under laboratory conditions for high precision metrology measurements. In addition to the comparability analysis of 3D and 2D calibration results, the influence caused by operator and machine is investigated for the 3D calibration method. Therefore, measurements were performed by three operators on three different CMMs. The CMMs are manufactured by Zeiss (UPMC 850, Prismo Ultra and Xenos) and are equipped with a VAST Gold probe and RT. The maximal permissible errors in three dimensions are $MPE_{UPMC\ 850} = 0.7\ \mu\text{m} + 0.17 \times L \times 10^{-5}$, $MPE_{Prismo\ Ultra} = 0.6\ \mu\text{m} + 0.2 \times L \times 10^{-5}$ and $MPE_{Xenos} = 0.2 + 0.3 \times L \times 10^{-6}$ with L in μm . Selected parameters for the 3D measuring procedure correspond to specifications given in [19] and are listed in table 1. Basic information of the 2D measurement is summarized in table 2. The stylus diameter is larger than the recommended one $d_D = 3.2030\ \text{mm}$ which is simultaneously touching both flanks at the nominal pitch diameter according to [4]. In the following, gathered raw data of both inspection methods are presented first. Afterwards, determined pitch diameters, the lead and flank angles obtained by 2D and 3D calibrations are compared to each other. Finally, the normalized errors considering both methods are presented.

4.1. Raw data

A gathered 3D point cloud is shown in figure 4 in combination with measured coordinates obtained by the standardized inspection. The point cloud of the 3D dataset is represented by greyish dots. Stylus sphere positions of the 2D calibration are illustrated true to scale as ruby coloured globes in two axial sections A – B and C – D. Even the measured 3D point cloud already gives an insight into the thread geometry, as both screw thread flanks are sufficiently well mapped due to $2 \times 40\ 800$ measured points (factor 2 is caused by reverse measuring). Radial and angular grid parameters are 0.5 mm and 1.67 mrad, respectively. Due to the high angular sampling rate, the 3D method enables the resolution of periodic form

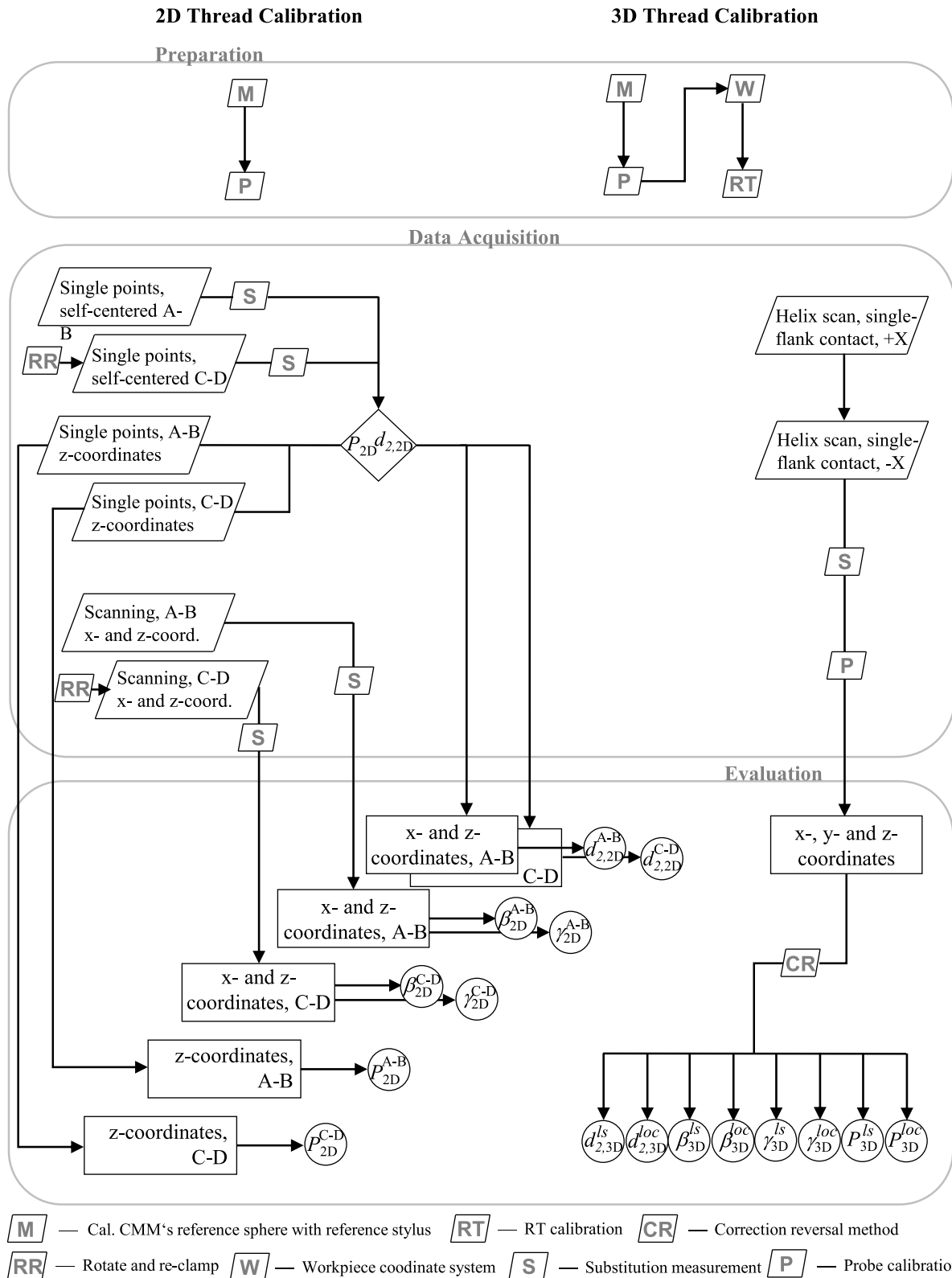


Figure 2. Flowchart to compare the 2D and 3D thread calibration steps.

deviations of up to approximately 190 oscillations per revolution. With the 2D method, however, only a maximum of one oscillation per revolution is resolvable. Compared to the 2D measuring method, the increased resolution capability

represents a considerable advantage. Small scaled periodic form deviations can be caused by the manufacturing process, e.g. when grinding, milling or turning, if for instance tool or workpiece axes are not supported in a sufficiently stable



Figure 3. Screw thread gauge used for the verification of the novel 3D inspection method.

manner and large static friction occurs. A further advantage is the separate probing of the two screw thread flanks. By measuring in single-point contact, form deviations are assigned to one single flank. The knowledge of where form deviations are exactly located enables the possibility to identify the reasons for their occurrence and the adjustment of the manufacturing process accordingly.

4.2. Pitch diameters

Pitch diameters of the $M64 \times 6$ external screw thread gauge determined by the 2D and 3D approach on three CMMs (UPMC 850, Prismo Ultra, Xenos) conducted by three operators (1, 2, 3) are shown in figure 4. In figure 5(a) 3D best-fit pitch diameters $d_{2,3D}^{ls}(z)$ derived by equation (6) with the least squares method (index *ls*) are presented in dependence of the z -coordinate aligned with the axis of rotation. The z -coordinate is negative because of the definition of the workpiece coordinate system. The origin is located on the top side of the screw thread and the normal vector of the surface points out of the workpiece as shown in figure 1(c). The presented results are exceeded by the nominal pitch diameter of $d_2^{\text{nominal}} = 60.103$ mm. However, the four curves show a high level of agreement over the entire range of the z -coordinate. Pitch diameters decrease by about 3 μm with

Table 1. Overview of measuring parameters used for 3D screw thread calibrations [19].

Parameter	Value
Air temperature	$(20.0 \pm 0.2)^\circ\text{C}$
Stylus tip diameter	(0.7815 ± 0.0013) mm
Material of stylus	Diamond-coated steel
Contact force	50 mN
Type of probing	Single-point contact
z -coordinate of P_C	(-62.3359 ± 0.9112) mm
Number of revolutions	9
Scanning speed	4 mm s^{-1}
Sampling rate	2 1/mm
Number of measuring tracks	6
Number of measuring points	$\approx 80\,000$

Table 2. Overview of measuring parameters used for the conventional 2D calibration following [4].

Parameter	Value
Air temperature	$(20.0 \pm 0.2)^\circ\text{C}$
Stylus diameter	(3.6125 ± 0.0001) mm
Material of stylus	Diamond-coated steel
Contact force	200 mN
Type of probing	Two-point contact
Measured gaps per section	9

increasing z -coordinate over the whole range, which corresponds to a taper angle of 0.0034° , which is nominally 0.0° .

The influence of using different CMMs is determined from the pitch diameter curves $d_{2,3D}^{ls}(z)$ UPMC 1 and $d_{2,3D}^{ls}(z)$ Prismo 1 by calculating the offsets and taking averages over the z -coordinate. Calibrations on two different CMMs by the same operator cause a difference of $0.08 \mu\text{m}$ for determined pitch diameters. The operator influence is estimated in the same way. The variation between $d_{2,3D}^{ls}(z)$ Xenos 2 and $d_{2,3D}^{ls}(z)$ Xenos 3 is $0.04 \mu\text{m}$, which is half of the CMM influence. The axes of figure 5(b) are scaled like in figure 5(a). Figure 5(b) shows 3D local pitch diameters $d_{2,3D}^{loc}(z)$ (dots) and 2D pitch diameters $d_{2,2D}(z)$ in axial sections A – B and C – D (symbols), calculated with equation (1). The same taper occurs as in figure 4(b), but the surface is shown in much more detail.

Figure 5(c) shows differences between mean values $d_{2,3D}^{loc}(z) - d_{2,3D}^{ls}(z)$ of pitch diameters (points) as well as those calculated for 2D pitch diameters in sections A – B and C – D $d_{2,2D}(z) - \overline{d_{2,3D}^{ls}}(z)$ (symbols). There is a nearly constant offset over the whole range of the z -coordinate. An explanation for this offset can be found by an interpretation of shape deviations on the surface. Because of the local diameters being smaller than the best-fit least squares diameters, it is obvious that the surface close to the pitch diameters is concavely shaped. Also, the 2D results support this interpretation. 2D measurements were performed in two-point contact, the probe slipped towards the root diameter, resulting in a smaller indicated value m than expected by an ideally shaped surface. In addition, a higher probing force is used for the 2D method than for the 3D method, so that the probe may be pressed

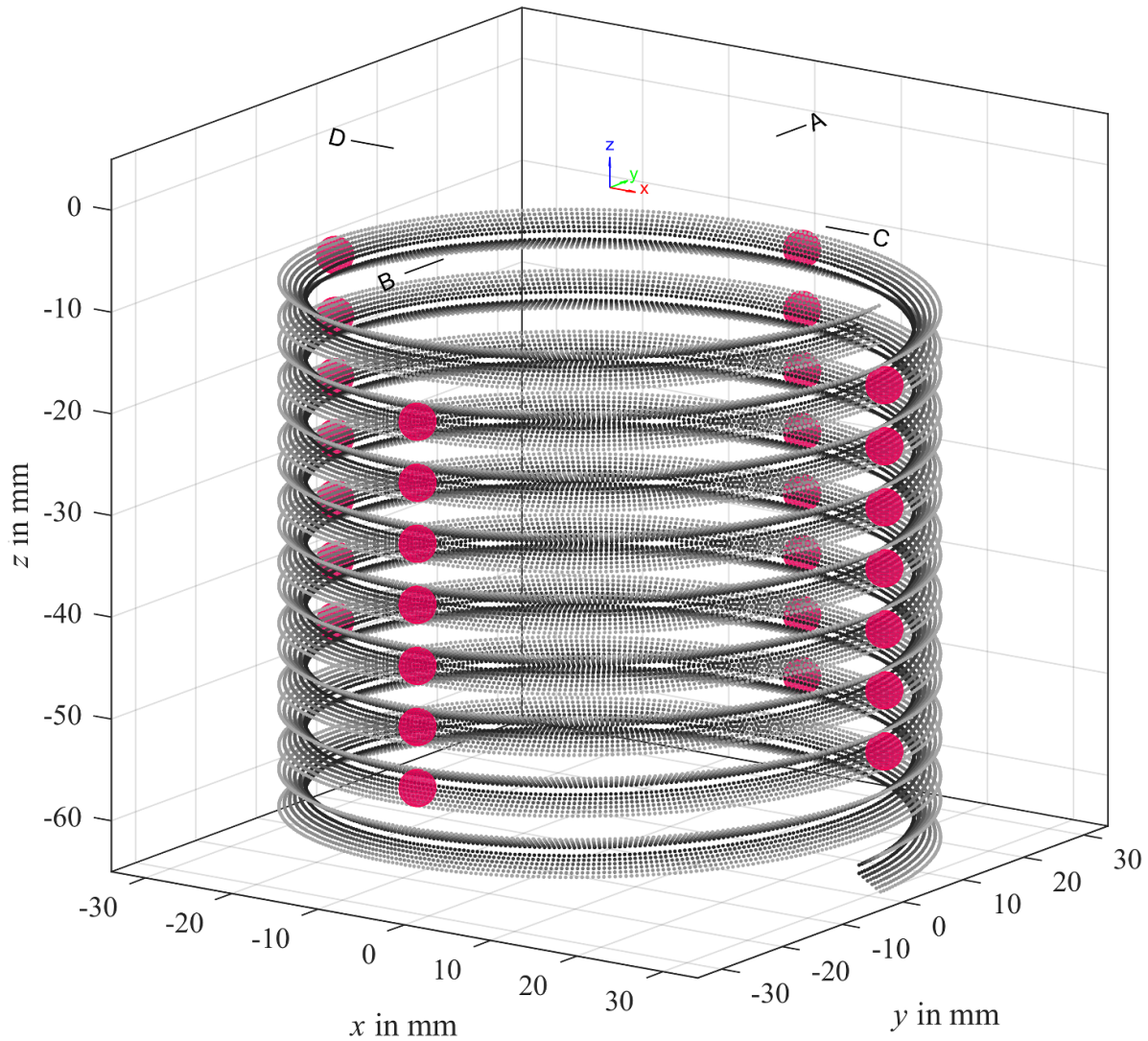


Figure 4. Measured point cloud (greyish coloured dots) resulting from the 3D calibration method and measured positions of the stylus sphere (true to size and ruby coloured) during a 2D calibration.

further into the workpiece in double-contact than necessary, which would also lead to smaller pitch diameters.

Another remarkable inconsistency appears in figure 5(b). 2D results deviate linearly increasing from local 3D results with increasing z -coordinates. The deviation is interpreted as an effect caused by the re-clamping of the screw thread gauge between measurements in section A – B and C – D, which leads to a change of the reference system, when 2D calibrations are performed. To re-clamp between two measurements thus should be avoided.

The conformity of local pitch diameters $d_{2,3D}^{loc}(z)$ derived by 3D calibrations in relation to the results from the standardized 2D method is examined by means of normalized errors E_n depending on the z -coordinate:

$$E_n(z) = \frac{d_{2,3D}^{loc}(z) - d_{2,2D}(z)}{\sqrt{U_{3D}^2 + U_{2D}^2}}, \quad (7)$$

where the mean values $\overline{d_{2,3D}^{loc}}(z)$ are locally considered over the four 3D calibrations. The uncertainties are $U_{3D} = 1 \mu\text{m}$ and $U_{2D} = 2 \mu\text{m}$, where the first value is estimated with PTB's virtual CMM tool conducting 2000 Monte Carlo simulations. These has been empirically tested regarding the convergence behaviour, which has shown that the results converge after approximately 500 runs. The second value is determined according to PTB's standard procedure for 2D screw thread gauge metrology with the GUM workbench (www.metrodata.de). If $0 \geq |E_n| \geq 1$ applies to the normalized error, then the results are considered consistent. The absolute value of normalized errors dependent on the z -coordinate according to equation (7) is shown in figure 6. Values referring to section A – B are marked as filled circles and those referring to section C – D are drawn as filled squares. The normalized error value is below 0.5 in the entire range. The exact numerical values for both sections are listed in table 3 as a function of the z -coordinate. The small normalized errors confirm the novel 3D calibration method on the example of

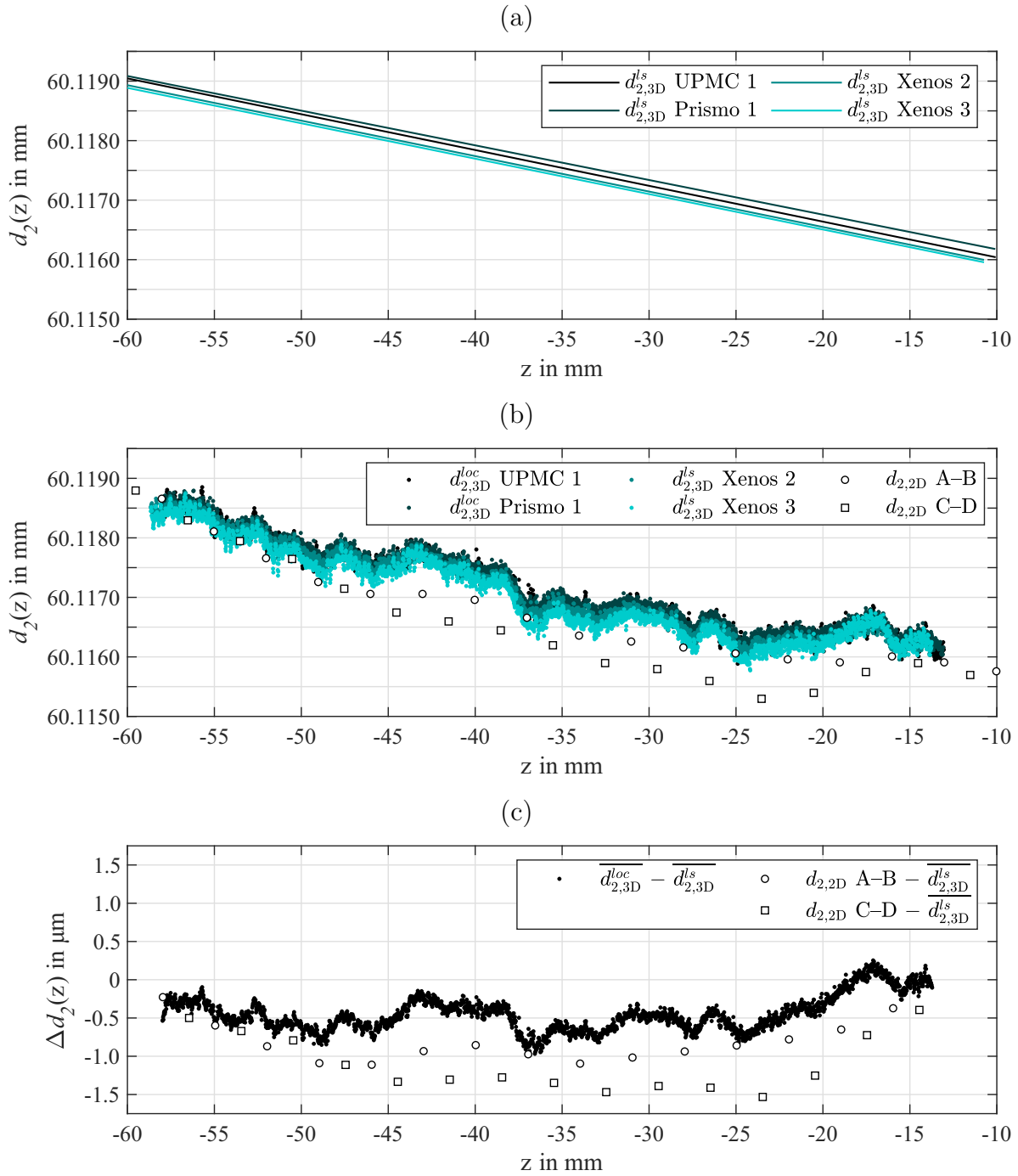


Figure 5. Evaluation results of four independent 3D screw thread gauge measurements performed on three different CMMs by three operators. (a) Best-fitting lines of the pitch diameter d_2 depending on the z -coordinate in alignment with the rotary axis of the screw thread gauge. (b) Corresponding local pitch diameter determined from 3D inspections (point clouds) and one 2D calibration (symbols). (c) Difference of pitch diameter mean values between 3D best-fit results shown in (a) and the local mean value respectively the 2D pitch diameter both illustrated in (b). Results marked with UPMC 1 and Prismo 1 are already published in [19].

the determination of pitch diameters presented here. Also, the influence of operator and CMM leads to $0.1 \mu\text{m}$ each, which is one order of magnitude smaller than the corresponding uncertainty. The maximum value of $|E_n| = 0.5$ and the accordance shown in figure 5 indicate the potential to further reduction of the measurement uncertainty in the future.

4.3. Lead and flank angles

In this section the local lead P_{3D}^{loc} and local flank angles β_{3D}^{loc} and γ_{3D}^{loc} are briefly compared to those obtained by means of the standardized 2D calibration procedure. Figure 7 shows the lead depending on the z -coordinate, which is in alignment with the screw threads rotary axis. The four results obtained

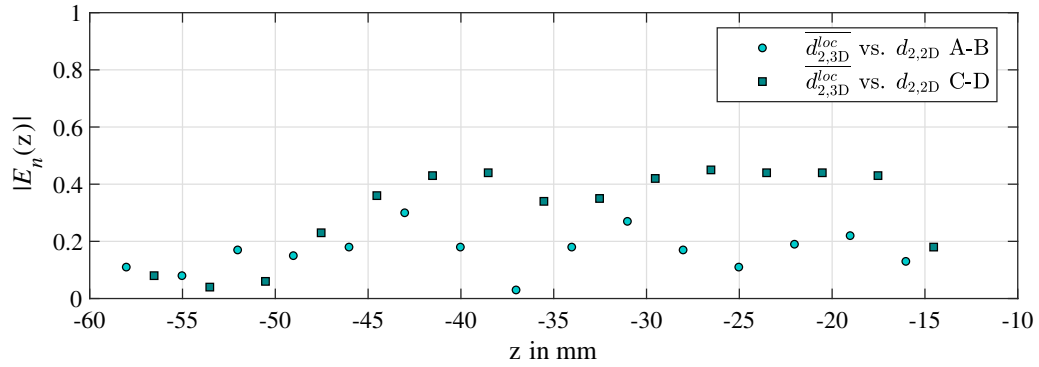


Figure 6. Normalized error $|E_n(z)|$ between d_2 derived by one 2D calibration and mean values of four different 3D calibrations in section A – B and C – D depending on the z -coordinate, which is in alignment with the rotary axis of the gauge.

Table 3. Normalized error $|E_n(z)|$ between d_2 derived by one 2D calibration and mean values of four different 3D calibrations depending on the z -coordinate in section A – B and C – D. The uncertainties are $U_{2D} = 2 \mu\text{m}$ and $U_{3D} = 1 \mu\text{m}$ (coverage factor $k = 2$ and level of confidence 95%).

z in mm	$ E_n(z) $ A – B	z in mm	$ E_n(z) $ C – D
-58.03	0.13	-56.53	0.08
-55.03	0.07	-53.53	0.03
-52.03	0.17	-50.53	0.05
-49.03	0.13	-47.53	0.22
-46.03	0.16	-44.53	0.35
-43.03	0.30	-41.53	0.42
-40.03	0.17	-38.53	0.44
-37.03	0.01	-35.53	0.33
-34.03	0.16	-32.53	0.33
-31.03	0.27	-29.53	0.41
-28.03	0.15	-26.53	0.44
-25.03	0.09	-23.53	0.42
-22.03	0.18	-20.53	0.43
-19.03	0.23	-17.53	0.44
-16.03	0.13	-14.53	0.18

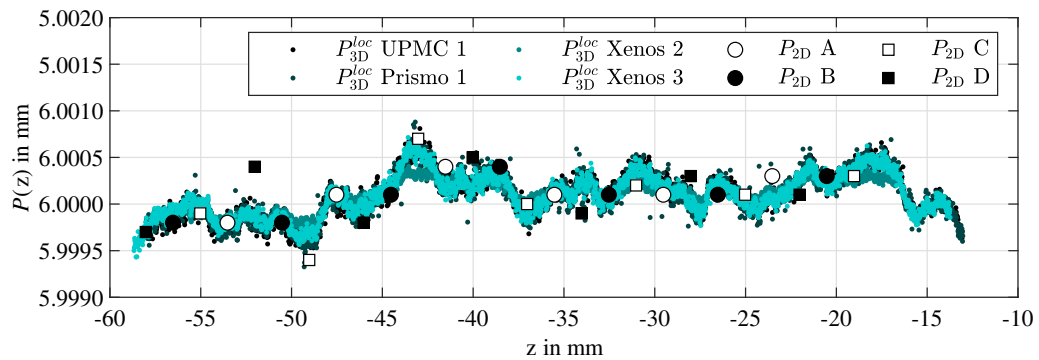


Figure 7. Evaluation results of the lead obtained by four independent 3D screw thread gauge measurements performed on three CMMs (UPMC, Prismo and Xenos) by three operators (1, 2 and 3).

by 3D calibrations (dots) equally progress with an increasing z -coordinate. Calculating the mean value over the four curves leads to a maximum standard deviation of $0.2 \mu\text{m}$ at $z \approx -43.2 \text{ mm}$ and a minimum of $0.003 \mu\text{m}$ at $z \approx -20.7 \text{ mm}$. If the average is also calculated over the z -coordinate, the standard deviation is $0.05 \mu\text{m}$. In contrast to the standard deviations mentioned above, this value corresponds less to a quality

criterion but rather to a kind of form deviation along the entire measured thread axis. The scatter of the results is five times larger than the associated uncertainty $U = 0.01 \mu\text{m}$, because form deviation is not yet taken into account. But it is intended to consider this contribution soon. However, the comparison to the 2D results shows good agreement between $P_{3D}^{loc}(z)$ and $P_{2D}(z)$, with one exception at $z \approx -52.1 \text{ mm}$. In the following

Table 4. Averaged screw thread determinants obtained by 2D and 3D calibrations. 2D results are averaged over one line of inspection (A, B, C or D) and 3D results are averaged over the entire range of the z -coordinate. In the two columns on the right side the standard deviation σ by averaging and the expanded uncertainty U is summarised.

Method		P in mm	σ in μm	U in μm
2D	A	5.99999	0.30	1.0
	B	6.00000	0.30	
	C	6.00001	0.40	
	D	6.00004	0.32	
3D		5.99993	0.05	0.01
Method		β in $^\circ$	σ in $'$	U in $'$
2D	A	-29.95858	0.092	3.0
	B	-29.96575	0.072	
	C	-29.95975	0.074	
	D	-29.96625	0.067	
3D		-29.96829	0.004	0.144
Method		γ in $^\circ$	σ in $'$	U in $'$
2D	A	29.92751	0.082	3.0
	B	29.92178	0.084	
	C	29.92625	0.087	
	D	29.91811	0.081	
3D		29.91260	0.004	0.196

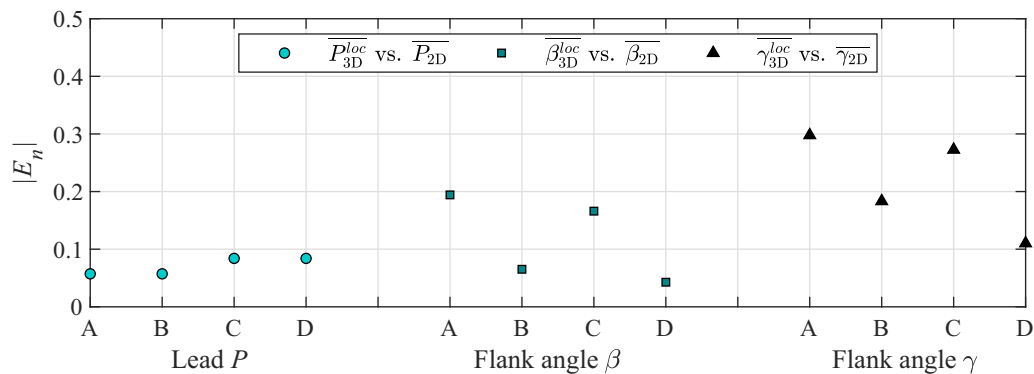


Figure 8. Normalized error $|E_n|$ derived by one 2D calibration and mean values of four different 3D calibrations for the determination of the pitch P and flank angles β and γ .

the results are averaged over the z -coordinate. The 3D results are also averaged over the four calibrations operated by three users on the different CMMs. Averaged calibration results, the standard deviation σ by averaging and the corresponding expanded uncertainty U are listed in table 4. The uncertainty is calculated with Monte-Carlo simulations as described in [19]. Note that all standard deviations by averaging are in the order or at least one order of magnitude smaller than the corresponding uncertainties. From the values in table 4, normalized errors following equation (7) are calculated and shown in figure 8. Again, normalized errors are clearly smaller than one with $|E_n| \leq 0.3$. $|E_n|$ of flank angle γ is largest in line A followed by line C. The other values are smaller than 0.2 as for the flank angle β (filled squares). Normalized errors of the lead P (filled circles) are even smaller $|E_n| < 0.1$, which indicates a high level of agreement between the 2D and 3D screw thread calibration method. Another result that supports the verification of the applied procedure. For a final conclusion, the numbers identified in this section are briefly summarised.

The analysis of the local pitch diameters at the beginning of this section has shown that the machine influence is $0.08 \mu\text{m}$. Changing the operator effects the pitch diameter even less and amounts to a deviation of $0.04 \mu\text{m}$. When examining the lead, the two influences were not separated, resulting in deviations between $0.003 \mu\text{m}$ and $0.2 \mu\text{m}$. Furthermore, the normalised errors between 3D and 2D results were determined. The result for the local pitch diameter is $|E_n| < 0.5$, for the local flank angles $|E_n| < 0.3$ and the local lead $|E_n| < 0.1$. All normalised errors are significantly smaller than 1, which means a high level of agreement between 2D and 3D results. Therefore, the 3D screw thread calibration method is considered to be confirmed.

5. Conclusion and outlook

A new 3D calibration method was verified with respect to a standardized 2D procedure. The presented examples have shown that the operator influence and the influence of different

CMMs on the determined pitch diameter is in both cases approximately 0.1 μm , which is within the uncertainty. Thus, the new 3D procedure enables a high reproducibility of the results.

From 2D and 3D calibrations, normalized errors were calculated which are significantly smaller than 0.5, so the results are considered as conformed.

Work is in progress to extend the metrology approach for other helical parts such as worms and gears. In addition, the evaluation method applied here is currently being integrated into the TraCIM service by PTB for automated validation of metrology software [28, 29]. Individual 3D evaluation algorithms for helical machine elements can be certified by the TraCIM service in the near future.

Acknowledgments

We would like to thank Marlen Krause (PTB) and Achim Wedmann (PTB) for carrying out some of the calibrations shown here and for providing information about the 2D calibration procedure. We would also like to thank the three anonymous reviewers for the contributions to this manuscript.

ORCID iDs

A Przyklenk  <https://orcid.org/0000-0002-6405-2315>

S Schädel  <https://orcid.org/0000-0003-1221-2572>

M Stein  <https://orcid.org/0000-0001-8729-8310>

References

- [1] Screw thread gauging systems for acceptability: inch and metric screw threads (UN, UNR, UNJ, M and MJ) 2007-10 Beuth Verlag GmbH
- [2] Gewinde–Begriffe und Bestimmungsgrößen für zylindrische Gewinde 2002-05 Beuth Verlag GmbH
- [3] Metrisches ISO-Gewinde allgemeiner Anwendung—Teil 1: Nennmaße für Regelgewinde; Gewinde-Nenndurchmesser von 1 mm bis 68 mm 1999-11 Beuth Verlag GmbH
- [4] Determination of pitch diameter of parallel thread gauges by mechanical probing 2012 EURAMET e.V. Braunschweig
- [5] Kalibrieren von Messmitteln für geometrische Messgrößen, Kalibrieren von zylindrischen Gewinde-Einstelldornen, Gewinde-Lehrdornen und -Prüfdornen 2018 Physikalisch-Technische Bundesanstalt
- [6] ISO Ref 1996 General-Purpose Metric Screw Threads—Gauges and Gauging (International Organization for Standardization)
- [7] Kalibrieren von Messmitteln für geometrische Messgrößen, Kalibrieren von zylindrischen Gewinde-Einstellringen, Gewinde-Lehringen 2018 Physikalisch-Technische Bundesanstalt
- [8] Weckenmann A, Estler T, Peggs G and McMurtry D 2004 Probing systems in dimensional metrology *CIRP Annals* **53** 657–84
- [9] Yüksel I A, Kiliç T O, Sönmez K B and Ön Aktan S 2019 Comparison of internal and external threads pitch diameter measurement by using conventional methods and CMMs *19th Int. Congress of Metrology (CIM2019) (Paris/France, 24–26 september 2019)* (<https://doi.org/10.1051/metrology/201909001>)
- [10] Krause M 2017 Intercomparison report DKD-V 4.3: Nationaler DKD-Ringvergleich für Gewindemessgrößen: 28
- [11] Kosarevsky S 2010 Development of an algorithm to detect screw threads in planar point clouds *Int. J. Adv. Manuf. Technol.* **48** 267–72
- [12] Tong Q, Jiao C, Huang H, Li G, Ding Z and Yuan F 2014 An automatic measuring method and system using laser triangulation scanning for the parameters of a screw thread *Meas. Sci. Technol.* **25** 035202
- [13] Lotze W and Will H-J 1991 Principle, theory and software for a new method of screw thread measurement by optical coordinate measuring systems *Measurement* **9** 153–6
- [14] Hong E, Zhang H, Katz R and Agapiou J S 2012 Non-contact inspection of internal threads of machined parts *Int. J. Adv. Manuf. Tech.* **62** 221–9
- [15] Kosarevsky S and Latypov V 2013 Detection of screw threads in computed tomography 3D density fields *Measurement Science Review* **13** 292-97
- [16] National Physical Laboratory 2010 NPL notes on screw gauges
- [17] Neuschaefer-Rube U, Neugebauer M, Ehrig W, Bartscher M and Hilpert U 2008 Tactile and optical microsensors: test procedures and standards *Meas. Sci. Technol.* **19** 084010
- [18] Primožič Merkač T and Ačko B 2010 Thread gauge calibration for industrial applications *Strojnicki vestnik—J. Mech. Eng.* **56** 637–43
- [19] Schädel S, Wedmann A and Stein M 2019 Advanced screw thread metrology using an areal measuring strategy and a holistic evaluation method *Meas. Sci. Technol.* **30** 075009
- [20] VDI/VDE-Gesellschaft Mess- und Automatisierungstechnik 2011 *Fertigungsmesstechnik 2020: Technologie-Roadmap für die Messtechnik in der industriellen Produktion* VDI-Verlag GmbH, Düsseldorf
- [21] Imkamp D, Berthold J, Heizmann M, Kniel K, Manske E, Peterek M, Schmitt R, Seidler J and Sommer K-D 2016 Challenges and trends in manufacturing measurement technology—the ‘Industrie 4.0’ concept *J. Sens. Sens. Syst.* **5** 325–35
- [22] Schädel S, Przyklenk A, Stein M, Kniel K and Manske E 2020 Ganzheitliche Kalibrierung von Gewinden auf Basis eines dreidimensionalen Ansatzes *Tech. Mess.* **87** 16–21
- [23] Schädel S 2020 *Neuartiges Messverfahren zur 3D-Gewindekalibrierung unter Verwendung einer flächenhaften Messstrategie und eines ganzheitlichen Auswertalgorithmus Dissertation* TU Ilmenau Ilmenau
- [24] Donaldson R R 1972 Simple method for separating spindle error from test ball error *CIRP Ann.* **21** 125–6
- [25] Sourlier D 1995 Three dimensional feature independent bestfit in coordinate metrology Dissertation ETH-Zürich, Zürich
- [26] Meß T, Ullmann V and Manske E 2017 Ganzheitliche erfassung von gewinden als antwort auf gesteigerte messunsicherheitsanforderung VDI-Nachrichten ed *Messunsicherheit praxisgerecht bestimmen und Prüfprozesse in der industriellen Praxis* vol 2319 *VDI-Berichte* Düsseldorf (VDI Verlag GmbH) 207–15
- [27] Torsten M 2017 Der paarungsflankendurchmesser —untersuchung des begrifflichen umfeldes, der einflussgrößen und der bedeutung für die funktion, Technische Universität Ilmenau, Ilmenau
- [28] Forbes A B, Smith I M, Härtig F and Wendt K 2015 Overview of emp joint research project NEW06 ‘traceability for computationally intensive metrology *Series on Advances in Mathematics for Applied Sciences* vol 86 (Singapore: World Scientific) pp 164–70
- [29] Wendt K, Franke M and Härtig F 2015 Validation of CMM evaluation software using TraCIM *Series on Advances in Mathematics for Applied Sciences* vol 86 (Singapore: World Scientific) pp 392–9